

Geophysical Research Letters[®]



RESEARCH LETTER

10.1029/2021GL097259

Key Points:

- Key metrics of global ocean circulation (Antarctic Circumpolar Current transport, Atlantic Meridional Overturning Circulation strength, and Ocean Heat Content anomaly) acutely sensitive to an eddy energy dissipation timescale
- Modest variations in the dissipation timescale has a comparable effect to significant variations in the Southern Ocean wind forcing
- Constraints on the dissipation timescale critical to longtime integrations of ocean climate models such as paleoclimate scenarios

Supporting Information:

Supporting Information may be found in the online version of this article.

Correspondence to:

J. Mak,
julian.c.l.mak@googlemail.com

Citation:

Mak, J., Marshall, D. P., Madec, G., & Maddison, J. R. (2022). Acute sensitivity of global ocean circulation and heat content to eddy energy dissipation timescale. *Geophysical Research Letters*, 49, e2021GL097259. <https://doi.org/10.1029/2021GL097259>

Received 30 NOV 2021

Accepted 1 APR 2022

Author Contributions:

Conceptualization: J. Mak, D. P.

Marshall, J. R. Maddison

Data curation: J. Mak

Formal analysis: J. Mak, D. P. Marshall, G. Madec

Funding acquisition: D. P. Marshall, J. R. Maddison





Investigation: J. Mak, D. P. Marshall, G. Madec

Methodology: J. Mak, D. P. Marshall, G. Madec, J. R. Maddison

© 2022. The Authors.

This is an open access article under the terms of the [Creative Commons Attribution License](https://creativecommons.org/licenses/by/4.0/), which permits use, distribution and reproduction in any medium, provided the original work is properly cited.

Acute Sensitivity of Global Ocean Circulation and Heat Content to Eddy Energy Dissipation Timescale

J. Mak^{1,2,3} , D. P. Marshall¹ , G. Madec⁴ , and J. R. Maddison⁵ 

¹Department of Physics, University of Oxford, Oxford, UK, ²Department of Ocean Science, Hong Kong University of Science and Technology, Hong Kong, Hong Kong, ³Center for Ocean Research in Hong Kong and Macau, Hong Kong University of Science and Technology, Hong Kong, Hong Kong, ⁴LOCEAN Laboratory, Sorbonne Universités (University Pierre et Marie Curie Paris 6)-CNRS-IRD-MNHN, Paris, France, ⁵School of Mathematics and Maxwell Institute for Mathematical Sciences, The University of Edinburgh, Edinburgh, UK

Abstract The global ocean overturning circulation, critically dependent on the global density stratification, plays a central role in regulating climate evolution. While it is well known that the global stratification profile exhibits a strong dependence to Southern Ocean dynamics and in particular to wind and buoyancy forcing, we demonstrate here that the stratification is also acutely sensitive to the mesoscale eddy energy dissipation timescale. Within the context of a global ocean circulation model with an energy constrained mesoscale eddy parameterization, it is shown that modest variations in the eddy energy dissipation timescale lead to significant variations in key metrics relating to ocean circulation, namely the Antarctic Circumpolar Current transport, Atlantic Meridional Overturning Circulation strength, and global ocean heat content, over long timescales. The results highlight a need to constrain uncertainties associated with eddy energy dissipation for climate model projections over centennial timescales and also for paleoclimate simulations over millennial timescales.

Plain Language Summary The ocean is populated by “eddies”, analogous to weather systems in the atmosphere, but occurring on much smaller scales of typically 10–100 km. Recent advances in our understanding of the circulation of the Southern Ocean, which connects all of the major ocean basins to the north, have revealed a crucial role for the energy balance of Southern Ocean eddies. In this paper, we show that the timescale over which energy is removed from Southern Ocean eddies has a dramatic impact on the following: (a) the strength of the Antarctic Circumpolar Current, the largest current in the global ocean; (b) the strength of the Atlantic meridional overturning circulation, responsible in part for the relatively mild climatic conditions over northwestern Europe; and (c) global ocean heat content, a key parameter in the global climate system. These results have significant implications for both past and future climates, and highlight the importance of combining observational, theoretical and modeling efforts to better understand and constrain the energy balance of ocean eddies.

1. Overview and Key Findings

Evolution of the ocean stratification plays a fundamental role in climate evolution, through the associated consequences for the global meridional overturning circulation. Reconstructions of past climate together with the use of numerical models have highlighted how shoaling and weakening of the Atlantic Meridional Overturning Circulation (AMOC), associated with changes in the deep/abyssal stratification, have important consequences for the global energy, oxygen and carbon cycles (e.g., Adkins, 2013; Bopp et al., 2017; Burke et al., 2015; Ferrari et al., 2014; Galbraith & de Lavergne, 2019; Jansen, 2017; Takano et al., 2018; Zhang & Vallis, 2013). In particular, Southern Ocean processes can exert a control on the global overturning circulation through the connectivity in the stratification (Newman et al., 2019).

It is known that the Southern Ocean stratification is primarily dependent on wind forcing (Toggweiler & Samuels, 1995; Toggweiler et al., 2006), buoyancy forcing (Hogg, 2010; Jansen, 2017; Morrison et al., 2011), and eddy dynamics (Bishop et al., 2016; Farneti et al., 2015; Munday et al., 2013). Focusing on mesoscale eddies, an extra complication arises since there are notable divergences in model response depending on how mesoscale eddies are represented, between whether they are represented explicitly or parameterized (Bishop et al., 2016; Farneti et al., 2015; Munday et al., 2013), and the form of the parameterization (Bishop et al., 2016; Farneti et al., 2015; Hofman & Morales Maqueda, 2011; Meredith et al., 2012; Munday et al., 2013; Viebahn & Eden, 2012). While

Project Administration: D. P. Marshall,
J. R. Maddison
Resources: D. P. Marshall
Software: J. Mak, G. Madec
Supervision: D. P. Marshall
Validation: J. Mak, G. Madec
Visualization: J. Mak
Writing – original draft: J. Mak, D. P.
Marshall, J. R. Maddison
Writing – review & editing: J. Mak, D.
P. Marshall, J. R. Maddison

the details of mesoscale eddy representation can have a disproportionately large influence on ocean climate sensitivity (Fox-Kemper et al., 2019), there have been advances on the eddy parameterization aspect, where the role of eddy energy in mesoscale eddy parameterizations is increasingly being studied (Eden & Greatbatch, 2008; Eden et al., 2014; Marshall & Adcroft, 2010; Marshall et al., 2012). Models with parameterized eddies employing eddy energy constrained eddy diffusivities or transport coefficients display improved model responses that are closer to the responses displayed in analogous high resolution models (Bachman, 2019; Jansen & Held, 2014; Jansen, Adcroft, et al., 2015; Jansen, Held, et al., 2015; Klöwer et al., 2018; Mak et al., 2017, 2018).

In particular, the GEOMETRIC parameterization (Mak et al., 2017, 2018; Marshall et al., 2012, 2017), effectively rescaling the standard Gent-McWilliams (Gent & McWilliams, 1990; Gent et al., 1995) eddy transport coefficient by the total eddy energy according to rigorous mathematical identities (Maddison & Marshall, 2013; Marshall et al., 2012), is supported by diagnoses of eddy resolving calculations (Bachman et al., 2017). A key impact of GEOMETRIC is to make the sensitivity of the Antarctic Circumpolar Current (ACC) and AMOC to changes in the Southern Ocean wind forcing closer to those in analogous high resolution models (Mak et al., 2018).

Since there is a link between eddy energy and the degree of feedback arising from the eddies, the mesoscale eddy energy dissipation timescale is expected to play an important role. Following the line of argument in Marshall et al. (2017), if more energy is drained from the mesoscale eddy field, the mesoscale eddy field and the associated eddy form stress weakens. The Ekman overturning cell then steepens the isopycnals until there is sufficient baroclinic instability for the associated eddy form stress to balance the surface wind stress. By thermal wind shear relation, increased ACC transport leads to steeply tilting isopycnals in the Southern Ocean that, through the connectivity in the stratification profiles, can have an influence on the global pycnocline depth and stratification, certainly over long timescales. The work of Marshall and Johnson (2017) provides a prediction between the vertical extents of the AMOC and the ACC that, assuming thermal wind shear relation and appropriate levels of no motion, becomes a relation between the corresponding transports. The prediction there is that an increased ACC transport, with corresponding deepening of the Southern Ocean stratification, leads to a deepening of the AMOC extent, implying an increased AMOC transport. A deeper pycnocline and increased AMOC transport will additionally suggest that the ocean is more susceptible in taking up heat through the isopycnal transport pathways, suggesting an increase in Ocean Heat Content (OHC).

In summary, the theoretical expectation here is that decreasing the mesoscale eddy energy dissipation timescale (i.e., increasing eddy energy dissipation) would lead to an increase in the ACC transport, increase in the AMOC strength as well as the OHC—and vice-versa—all attributed to changes in the Southern Ocean stratification driving changes in the global pycnocline depth over long timescales, enabled by the connectivity of the stratification profiles. The primary focus of the present work is to demonstrate and quantify the extent and magnitude of the influence of eddy energy dissipation timescale on the aforementioned key ocean climatological metrics. A key finding here is that a modest variation in the eddy energy dissipation timescale has a comparable effect to significant variations in the present day Southern Ocean wind forcing on the modeled ACC transport, AMOC strength, and the global integrated OHC anomaly (Figure 1, Figure 3 and Table 1), attributed primarily to changes in the global pycnocline depth. While the Southern Ocean wind forcing is not expected to vary as dramatically to the degree investigated in this work, the extent of the plausible mesoscale eddy energy dissipation timescale is not known, due to a lack of theoretical and observation constraints currently available. The results here thus highlight a crucial need to combine theoretical, modeling, and observational efforts to constrain the uncertainties in eddy energy dissipation, not only from a theoretical point of view for understanding, but also for practical purposes in constraining uncertain model parameters for numerical models used in climate projections and paleoclimate reconstructions.

2. Method and Model Description

The principal focus here is on quasi-equilibrium sensitivities of the global ocean overturning circulation to the eddy energy dissipation timescale. While one might consider employing an eddy resolving ocean model for such a study, the associated computational costs are prohibitive. Thus we employ a model with parameterized eddies, and utilize the Nucleus for European Modeling of the Ocean (NEMO, v3.7dev r8666; Madec, 2008) in the global configuration (ORCA) with realistic bathymetry, employing the tripolar ORCA grid (Madec & Imbard, 1996) and the LIM3 ice model (Rousset et al., 2015). The present ORCA1 model has a nominal horizontal resolution of

1°, employs 46 uneven vertical levels, and is initialized with WOA13 climatology (Locarnini et al., 2013; Zweng et al., 2013). The model employs the TEOS-10 equation of state (Roquet et al., 2015), with the atmospheric forcing modeled by the NCAR bulk formulae with normal year forcing (Large & Yeager, 2009). Sea surface salinity but not temperature restoration is included to reduce model drift.

An energetically constrained mesoscale eddy parameterization scheme is required, and for our investigation the GEOMETRIC parameterization for mesoscale eddies (Mak et al., 2018; Marshall et al., 2012) was chosen and implemented in NEMO (see Supporting Information S1 for implementation details). Briefly, GEOMETRIC computes a horizontally and temporally varying coefficient for eddy-induced advection (Gent & McWilliams, 1990; Gent et al., 1995) according to (cf. Equation 4 of Mak et al., 2018)

$$\kappa_{\text{gm}} = \alpha \frac{\int E \, dz}{\int (M^2/N) \, dz}, \quad (1)$$

where M and N are the horizontal and vertical buoyancy frequencies, α is a nondimensional tuning parameter (bounded in magnitude by 1), and E is the total (potential and kinetic) eddy energy. The depth-integrated eddy energy $\int E \, dz$ is provided by a parameterized eddy energy budget given by (cf. Equation 2 of Mak et al., 2018)

$$\frac{d}{dt} \int E \, dz + \underbrace{\nabla_H \cdot \left((\tilde{\mathbf{u}}^z - |c| \mathbf{e}_x) \int E \, dz \right)}_{\text{advection}} = \underbrace{\int \kappa_{\text{gm}} \frac{M^4}{N^2} \, dz}_{\text{source}} - \underbrace{\lambda \int (E - E_0) \, dz}_{\text{dissipation}} + \underbrace{\eta_E \nabla_H^2 \int E \, dz}_{\text{diffusion}} \quad (2)$$

The depth-integrated eddy energy is advected by the depth average flow $\tilde{\mathbf{u}}^z$ and propagated westward at the long Rossby wave phase speed $|c|$ (Chelton et al., 1998, 2011; Gill, 1982; Klocker & Marshall, 2014), has growth arising from slumping of mean density surfaces, and diffused in the horizontal (Grooms, 2015; Ni, Zhai, Wang, & Hughes, 2020; Ni, Zhai, Wang, & Marshall, 2020), with ∇_H denoting the horizontal gradient operator and η_E the associated eddy energy diffusivity. A linear dissipation of eddy energy at rate λ (but maintaining a minimum eddy energy level E_0) is utilized, so λ^{-1} is the eddy energy dissipation timescale of primary interest here. For this work, $\alpha = 0.04$ is prescribed, partially informed by the results of Poulsen et al. (2019), and $\eta_E = 500 \, \text{m}^2 \, \text{s}^{-1}$ is chosen. Although the Gent-McWilliams coefficient follows the prescription given in Equation 1, the isoneutral diffusion coefficient (Griffies, 1998) is kept constant at $1,000 \, \text{m}^2 \, \text{s}^{-1}$; while the two quantities are related to mesoscale turbulence, and there are studies that suggest how the two should be related (e.g., Abernathy et al., 2013; Smith & Marshall, 2009), for simplicity, we make the choice to fix the isoneutral diffusion coefficient, noting that changing this coefficient can also affect climatological responses (e.g., Jones & Abernathy, 2019; Pradal & Gnanadesikan, 2014). Values of the isopycnal slopes used to compute the parameterized eddy energy, eddy-induced advection and isoneutral diffusion are limited to 1/100 in the interior, and linearly decreased from the base of the model-mixed layer to zero at the surface to maintain no flux conditions.

Given the lack of constraints on the values and uncertainties associated with the eddy energy dissipation timescale λ^{-1} , we consider a plausible variation around some control value. With the Southern Ocean in mind, for simplicity we take a constant control eddy energy dissipation timescale of $\lambda^{-1} = 100$ days (around 3 months). It was empirically determined that six experiments with eddy energy dissipation timescale ranging from 60 to 160 days (around 2–5 months), in increments of 20 days (around 2/3 of a month) provided a sufficient coverage of the parameter space. The control experiment with $\lambda^{-1} = 100$ days (around 3 months) was first spun up for 1,500 years, after which the perturbation experiments were integrated for a further 1,600 years; see Figures S1–S4 in Supporting Information S1 for some of the resulting climatology. All metrics presented in this work were calculated from model outputs time-averaged over the model years 3500–3600.

3. Results

3.1. Sensitivity to the Eddy Energy Dissipation Timescale

The key metrics of interest here are the total ACC transport, AMOC strength, and the globally integrated OHC anomaly relative to the control calculation time-averaged over model years 3500–3600, respectively given as the transport through the model Drake passage, the transport over the top 1,000 m at the model 26°N on the Western side of the Atlantic, and the global integrated conservative temperature multiplied accordingly by the density

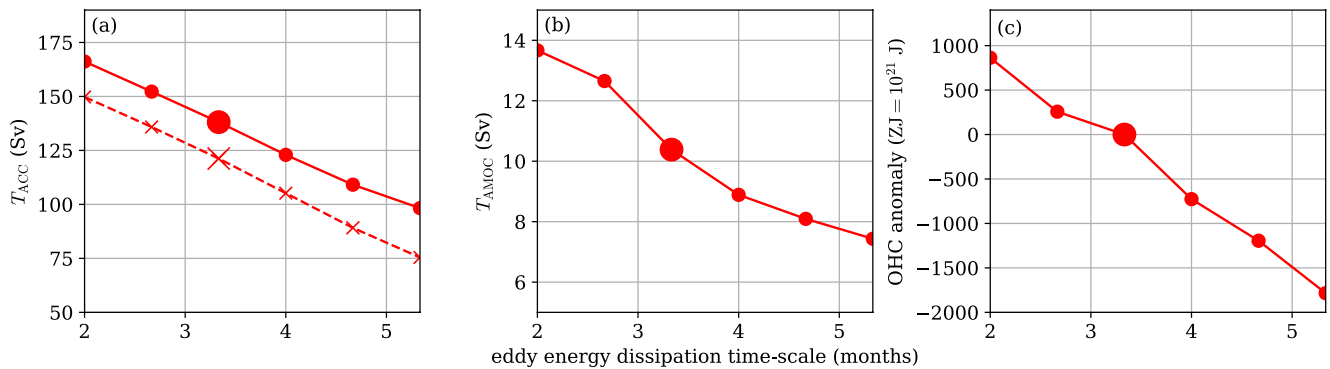


Figure 1. Diagnostics from the varying eddy energy dissipation time-scale experiments. Diagnostics are: (a) Antarctic Circumpolar Current transport (total in solid lines, thermal wind component in dashed lines); (b) Atlantic Meridional Overturning Circulation strength as transport over the top 1,000 m depth at 26° N on the Western side of the Atlantic; (c) domain-integrated Ocean Heat Content anomalies as solid lines, where the anomalies are relative to the control calculation diagnosed at the same analysis time period, with the value of 21,300 ZJ. The larger marker denotes the control calculation.

and heat capacity. A depth-independent ACC transport was computed through a depth-integral of the bottom velocity, and a thermal wind component of the ACC is the difference between the total and depth-independent ACC transport described above (cf. Abernathy et al., 2011; Munday et al., 2013). Figure 1 compares these metrics diagnosed from experiments varying the eddy energy dissipation timescale. Increasing the dissipation timescale (i.e., decreased damping of the eddies) leads to a substantial decrease in the ACC transport, AMOC strength, and total OHC anomaly—and vice-versa—which can be attributed to shifts in the global pycnocline depth, consistent with theoretical arguments (Marshall & Johnson, 2017; Marshall et al., 2017). To quantify the trends, Table 1 documents the numerical values obtained from a linear regression analysis of the data presented in Figure 1. The implied sensitivities to the eddy energy dissipation timescale are significant, at around 20 Sv of ACC transport, 2 Sv of AMOC strength and 800 ZJ of OHC anomaly change per 30 days (1 month) variation. In particular, we note that the changes in the OHC anomalies found in postindustrial period reconstructions (Cheng et al., 2017, 2019; Levitus et al., 2012; Zanna et al., 2019) are typically on the order of 10^{23} J (100 ZJ), while the changes to total OHC associated with the uncertainties in eddy energy dissipation timescale here can be an order of magnitude larger (10^{24} J).

The distribution of the lateral depth-integrated OHC for varying the eddy energy dissipation timescale is shown in Figure 2. Varying the eddy energy dissipation timescale leads to a significant global change in the OHC anomalies, attributed mainly to the changes in pycnocline depth (Figures S6–S9 in Supporting Information S1). Note also that the changes appear to be most significant over the Southern Ocean and in the Atlantic basin, attributed to significant changes in the AMOC as well as the overturning within the Southern Ocean (Figures S3 and S4 in Supporting Information S1).

Here, changing the eddy energy dissipation timescale affects the total eddy energy E , which in turn impacts the Gent-McWilliams coefficient κ_{gm} . While the significant changes to global OHC and circulation arising from changing κ_{gm} has been noted before (e.g., Zhang & Vallis, 2013), the fundamental difference here is that the sensitivities are arising through uncertainties in the eddy energy dissipation that happens to impact the Gent-McWilliams parameter, and the eddy energy dissipation is a process that, in principle, is more amenable to be constrained by theoretical, numerical or observational means.

3.2. Sensitivity to Southern Ocean Wind Forcing

For completeness, experiments varying Southern Ocean wind forcing are also performed. The zonal wind stress over the Southern Ocean region within the model is amplified instead of the imposed zonal wind speed, so that any modifications to the ocean surface evaporation and turbulent fluxes as calculated through the bulk formulae occur through changes to the ocean state rather than the imposed wind forcing. Two sets of perturbation experiments are performed: (a) a κ_{gm} that is varying in the horizontal and in time as given by Equation 1, with no further retuning (denoted GEOM), and (b) a prescribed κ_{gm} diagnosed from the last 100 years of the control spin-up (denoted GM), still spatially varying, but is now time-independent.

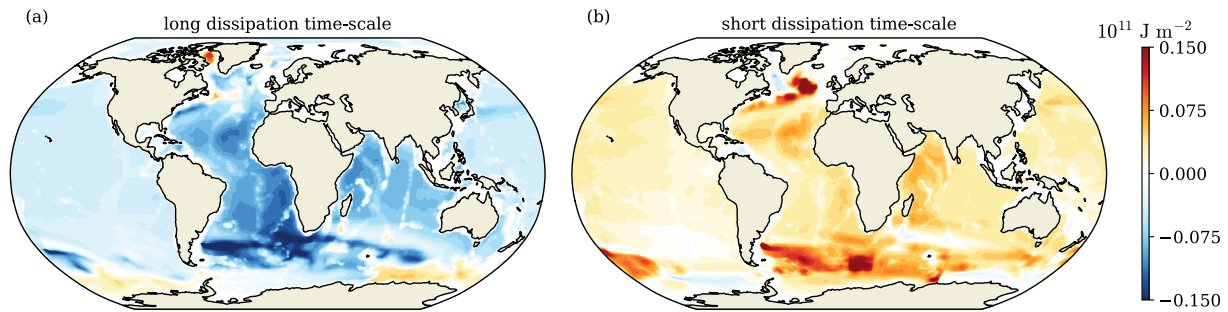


Figure 2. Depth-integrated ocean heat content anomaly relative to the control calculation diagnosed at the same analysis period for varying dissipation experiments. (a) $\lambda^{-1} = 160$ days (around 5 months). (b) $\lambda^{-1} = 60$ days (around 2 months).

Figure 3 shows the sensitivities of the same global ocean climatological metrics to changes in the imposed Southern Ocean wind forcing, and Table 1 documents the numerical values obtained from a linear regression analysis of the data presented in Figure 3. While the total ACC transport increases with wind forcing, the ACC thermal wind transport in the GEOM calculations is relatively insensitive to changes in the wind forcing (with a diagnosed trend of around 2 Sv per factor of Southern Ocean wind forcing variation in GEOM, compared to a value of around 20 Sv displayed by the GM experiments), demonstrating the eddy saturation phenomenon (Bishop et al., 2016; Farneti et al., 2015; Hallberg & Gnanadesikan, 2006; Meredith & Hogg, 2006; Munday et al., 2013). The corresponding AMOC strength in the GEOM calculations also display a reduced sensitivity to changes in the Southern Ocean wind forcing relative to the GM case (with a diagnosed trend of around 4 Sv in GEOM compared to 5 Sv in GM per factor of Southern Ocean wind forcing increase), and is related to the phenomenon of eddy compensation (Bishop et al., 2016; Farneti et al., 2015; Gent & Danabasoglu, 2011; Hofman & Morales Maqueda, 2011; Meredith et al., 2012; Munday et al., 2013; Viebahn & Eden, 2012). The aforementioned sensitivities coincide with a weaker sensitivity of the global pycnocline depth to changes in Southern Ocean wind forcing (Mak et al., 2018; Marshall et al., 2017). As with the varying eddy energy dissipation experiments, the OHC anomalies are particularly significant over the Southern Ocean and the Atlantic basin (Figure S5 in Supporting Information S1). In the present case of varying wind stress, however, the notable variations in the OHC anomalies are attributed to significant changes in the abyssal watermass properties (Figures S6–S9 in Supporting Information S1). The observed changes in the watermass properties may perhaps be attributed to a modified sea ice extent (Figure S10 in Supporting Information S1) via changes in the sea ice export by the wind, leading to changes in deep water formation and abyssal watermass properties, analogous to the mechanism proposed in Ferrari et al. (2014) and Burke et al. (2015).

Table 1

Linear Regression of the Diagnosed Global Ocean Climatological Metrics for Varying Eddy Energy Dissipation Timescale and Varying Southern Ocean Wind Forcing Amplification Factor

Metric	Varying dissipation timescale λ^{-1} (per 30 days/1 month)	Varying Southern Ocean wind forcing τ_0 (per amplification factor)
T_{ACC} (total, Sv)	$-20.74 \lambda^{-1} + 207.20$ (GEOM)	$+15.44 \tau_0 + 119.32$ (GEOM) $+32.04 \tau_0 + 97.22$ (GM)
T_{ACC} (thermal, Sv)	$-22.61 \lambda^{-1} + 195.69$ (GEOM)	$+2.07 \tau_0 + 114.64$ (GEOM) $+19.73 \tau_0 + 90.57$ (GM)
T_{AMOC} (Sv)	$-1.99 \lambda^{-1} + 17.47$ (GEOM)	$+3.82 \tau_0 + 6.41$ (GEOM) $+5.07 \tau_0 + 5.41$ (GM)
OHC anomaly (ZJ = 10^{21} J)	$-785.17 \lambda^{-1} + 2,448.13$ (GEOM)	$+524.82 \tau_0 - 940.31$ (GEOM) $+1,158.80 \tau_0 - 1872.50$ (GM)

Note. The first coefficient denotes trends with varying parameter of interest in this work.

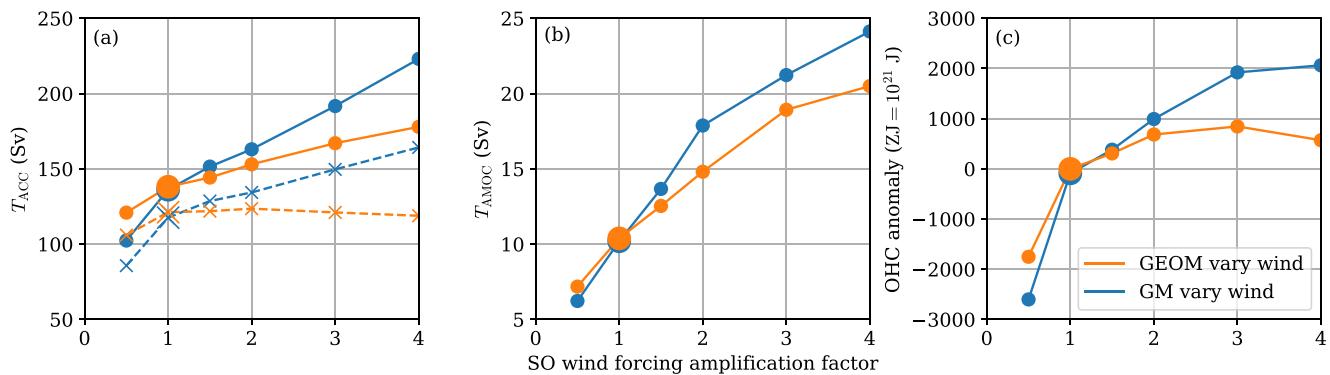


Figure 3. Diagnostics from the varying Southern Ocean wind stress experiments (with GEOM and GM calculations in orange and blue, respectively), showing: (a) Antarctic Circumpolar Current transport (total in solid lines, thermal wind component in dashed lines); (b) Atlantic Meridional Overturning Circulation strength as transport over the top 1,000 m depth at 26°N on the Western side of the Atlantic; (c) domain-integrated ocean heat content anomalies as solid lines, where the anomalies are relative to the control calculation diagnosed at the same analysis time period, with the value of 21,300 ZJ. The larger marker denotes the control calculation.

4. Summary and Outlooks

The present work demonstrates that, within the context of a global configuration ocean model with an energetically constrained mesoscale eddy parameterization, modest and perhaps not implausible variations in the mesoscale eddy energy dissipation timescale translate to significant sensitivities of the diagnosed ACC transport, AMOC strength, and the global OHC over long timescales in the modeled ocean. The physical reasons for the sensitivity is that modifying the eddy energy dissipation leads to changes in the mesoscale eddy dynamics in the Southern Ocean, modifying the Southern Ocean stratification, and in turn lead to significant changes to the global ocean stratification over long timescales. In particular, changes to the globally integrated OHC anomalies can vary by up to an order of magnitude larger than for reconstructions for total OHC for the anthropogenic period (Cheng et al., 2017, 2019; Levitus et al., 2012; Zanna et al., 2019) and comparable to the end of 21st projections under the Representative Concentration Pathways scenarios (see figure in Cheng et al., 2019). The sensitivity of the aforementioned key ocean climatological metrics to the eddy energy dissipation timescale is found to be significant: comparing the trend values documented in Table 1, the sensitivities of the total ACC transport, AMOC strength, and the global OHC per 30 days (1 month) of the eddy energy dissipation timescale are comparable to per multiplicative factor change in the Southern Ocean wind forcing. While the changes in the Southern Ocean wind forcing are not expected to vary to the extent considered in this work (e.g., Lin et al., 2018), there are no strong theoretical, numerical or observational constraints on the eddy energy dissipation timescale and its distribution (but see next paragraph on studies toward constraining the energy fluxes of the contributing processes). There is thus a need to combine and dedicate theoretical, modeling and observational efforts to constrain the uncertainties in the eddy energy dissipation timescale, given the impact the associated uncertainties can have.

In the present work the eddy energy dissipation is linear (cf., Klymak, 2018) with a timescale that is a prescribed constant in space and time. One particular consequence of a prescribed spatially constant eddy energy dissipation timescale may be seen in Figure 4, which shows the total (kinetic and potential) eddy energy diagnosed from a high-resolution global configuration model and from the control experiment here. While the eddy energy signature displays some similarities in terms of spatial patterns in the Southern Ocean and Western Boundary Current regions, there is clearly room for improvement for the parameterized case. For example, the eddy energy signature in the parameterized case is too weak in the Western Boundary Currents and in the equatorial region, attributed to the fact that the spatially constant eddy energy dissipation timescale was chosen with the Southern Ocean in mind, and is probably too short for the ocean basin regions.

The mesoscale eddy energy dissipation timescale is expected to be a more complicated function than the choice taken here and, fundamentally, should depend on a wide variety of dynamical processes, such as bottom drag (e.g., Ruan et al., 2021; Sen et al., 2008), nonpropagating form drag (Klymak, 2018, 2021), return to mean-flow (e.g., Bachman, 2019; Jansen et al., 2019) scattering into internal waves (e.g., MacKinnon et al., 2017; Melet et al., 2015; Nikurashin et al., 2013; Sutherland et al., 2019; Yang et al., 2018), loss of balance (e.g., Barkan et al., 2017; Molemaker et al., 2005; Rocha et al., 2018), and eddy damping by the wind (e.g., Rai et al., 2021;

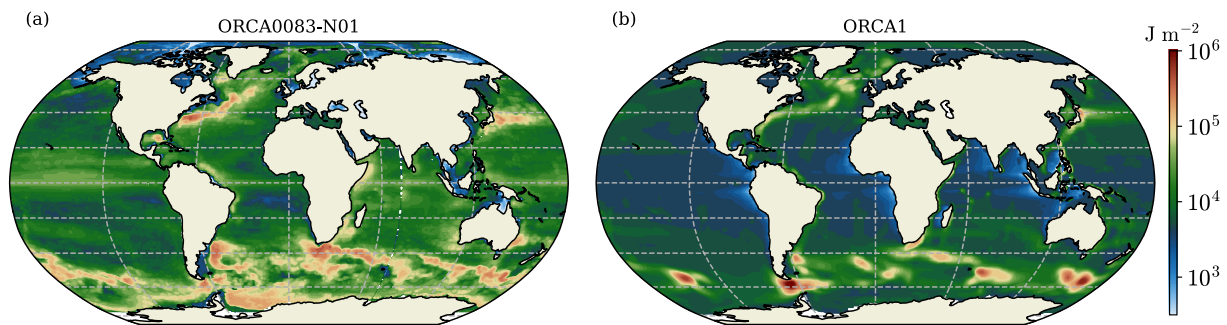


Figure 4. Depth-integrated total (kinetic and potential) eddy energy density (in units of J m^{-2}), diagnosed from (a) the high resolution ORCA0083-N01 calculation with explicit eddies, and (b) from the GEOM control calculation.

Xu et al., 2016). Although the challenges in constraining the uncertainties in the eddy energy dissipation timescale are formidable, the observed/diagnosed eddy energy signature can perhaps act as a target toward efforts to constrain the aforementioned unknowns, highlighting the potential for further research relating to ocean energetic pathways and its consequences for climate evolution (see e.g., Ruan et al., 2021 for a recent review of research relating to ocean eddy energy pathways).

For completeness, we note that even with the use of the simple linear eddy energy dissipation timescale here, the resulting dissipation of the depth-integrated total eddy energy in the present parameterization seems to follow an approximately log-normal distribution when considered over the globe (cf. Perason & Fox-Kemper, 2018, but for horizontal eddy kinetic energy), although with deviations particularly with increasing Southern Ocean wind forcing and a decreased eddy energy dissipation timescale, which both lead to a skew towards larger dissipation rates (see Figure S11 in Supporting Information S1).

While the present results have been obtained with the GEOMETRIC parameterization for mesoscale eddies (Mak et al., 2018), given the fundamental link between the eddy energy dissipation timescale, eddy energy, and the resulting eddy-induced circulation, the sensitivities of key ocean climatological metrics to the eddy energy dissipation can be expected to carry over to models with other eddy energy-based parameterization of mesoscale eddies (e.g., Jansen, Adcroft, et al., 2015; Bachman, 2019) and to models in which eddies are resolved explicitly. However, we expect that the magnitudes of the sensitivities of the key metrics to the eddy energy dissipation timescale may differ. While the present work has focused on quasi-equilibrium calculations, similar conclusions, but with reduced magnitudes of the sensitivities, are obtained on centennial timescales.

Finally, we suggest that the present work has significant implications for the design of paleoclimate model simulations, such as in the Paleoclimate Modeling Intercomparison Project calculations (Kageyama et al., 2018), given the long time-scales inherently required for the related simulations. The impact of GEOMETRIC, and the eddy energy dissipation time scale, on future climate projections and paleoclimates will be investigated and reported in due course.

Data Availability Statement

This work utilizes the Nucleus for European Modelling of the Ocean model (NEMO, v3.7dev r8666; <https://www.nemo-ocean.eu/>). The data and scripts used for generating the plots in this article are available at <https://doi.org/10.5281/zenodo.5732755>.

References

- Abernathy, R., Ferreira, D., & Klocker, A. (2013). Diagnostics of isopycnal mixing in a circumpolar channel. *Ocean Modelling*, 72, 1–16. <https://doi.org/10.1016/j.ocemod.2013.07.004>
- Abernathy, R., Marshall, J., & Ferreira, D. (2011). The dependence of Southern Ocean meridional overturning on wind stress. *Journal of Physical Oceanography*, 41, 2261–2278. <https://doi.org/10.1175/JPO-D-11-023.1>
- Adkins, J. F. (2013). The role of deep ocean circulation in setting glacial climates. *Paleoceanography*, 28, 539–561. <https://doi.org/10.1002/palo.20046>
- Bachman, S. D. (2019). The GM+E closure: A framework for coupling backscatter with the Gent and McWilliams parameterization. *Ocean Modelling*, 136, 85–106. <https://doi.org/10.1016/j.ocemod.2019.02.006>

Acknowledgments

This work was funded by the UK Natural Environment Research Council grant NE/R000999/1 and utilized the ARCHER UK National Supercomputing Service. JM also acknowledges financial support from the Hong Kong RGC Early Career Scheme 2630020 and the Center for Ocean Research in Hong Kong and Macau, a joint research center between the Qingdao National Laboratory for Marine Science and Technology and Hong Kong University of Science and Technology. The authors would like to thank Andrew Coward for providing access to the ORCA0083-N01 data set through the ARCHER RDF service, Xiaoming Zhai for discussions relating to observational inferences of the eddy energy residence timescale, George Nurser for discussions in relation to the GEOMETRIC implementation and outlooks, and Baylor Fox-Kemper as well as an anonymous referee for their review comments that led to improvements to the article.

- Bachman, S. D., Marshall, D. P., Maddison, J. R., & Mak, J. (2017). Evaluation of a scalar transport coefficient based on geometric constraints. *Ocean Modelling*, 109, 44–54. <https://doi.org/10.1016/j.ocemod.2016.12.004>
- Barkan, R., Winters, K. B., & McWilliams, J. C. (2017). Stimulated imbalance and the enhancement of eddy kinetic energy dissipation by internal waves. *Journal of Physical Oceanography*, 47, 181–198. <https://doi.org/10.1175/JPO-D-16-0117.1>
- Bishop, S. P., Gent, P. R., Bryan, F. O., Thompson, A. F., Long, M. C., & Abernathy, R. P. (2016). Southern Ocean overturning compensation in an eddy-resolving climate simulation. *Journal of Physical Oceanography*, 46, 1575–1592. <https://doi.org/10.1175/JPO-D-15-0177.1>
- Bopp, L., Resplandy, L., Untersee, A., Le Mezo, P., & Kageyama, M. (2017). Ocean (de)oxygenation from the last glacial maximum to the twenty-first century: Insights from Earth system models. *Philosophical Transactions of the Royal Society A: Mathematical, Physical and Engineering Sciences*, 375, 20160323. <https://doi.org/10.1098/rsta.2016.0323>
- Burke, A., Stewart, A. L., Adkins, J. F., Ferrari, R., Jansen, M. F., & Thompson, A. F. (2015). The glacial mid-depth radiocarbon bulge and its implications for the overturning circulation. *Paleoceanography*, 30, 1021–1039. <https://doi.org/10.1002/2015PA002778>
- Chelton, D. B., de Szoeke, R. A., Schlax, M. G., El Naggar, K., & Siwertz, N. (1998). Geographical variability of the first baroclinic Rossby radius of deformation. *Journal of Physical Oceanography*, 28, 433–460. [https://doi.org/10.1175/1520-0485\(1998\)028<0433:gvotfb>2.0.co;2](https://doi.org/10.1175/1520-0485(1998)028<0433:gvotfb>2.0.co;2)
- Chelton, D. B., Schlax, M. G., & Samelson, R. M. (2011). Global observations of nonlinear mesoscale eddies. *Progress in Oceanography*, 91, 167–216. <https://doi.org/10.1016/j.pocan.2011.01.002>
- Cheng, L., Abraham, J., Hausfather, Z., & Trenberth, K. E. (2019). How fast are the oceans warming? *Science Advances*, 363, 128–129. <https://doi.org/10.1126/science.aav7619>
- Cheng, L., Trenberth, K. E., Fasullo, J., Boyer, T., Abraham, J., & Zhu, J. (2017). Improved estimates of ocean heat content from 1960 to 2015. *Science Advances*, 3, e1601545. <https://doi.org/10.1126/sciadv.1601545>
- Eden, C., Czeschel, L., & Olbers, D. (2014). Toward energetically consistent ocean models. *Journal of Physical Oceanography*, 44, 3160–3184. <https://doi.org/10.1175/jpo-d-13-0260.1>
- Eden, C., & Greatbatch, R. J. (2008). Towards a mesoscale eddy closure. *Ocean Modelling*, 20, 223–239. <https://doi.org/10.1016/j.ocemod.2007.09.002>
- Farneti, R., Downes, S. M., Griffies, S. M., Marsland, S. J., Behrens, E., Bentsen, M., et al. (2015). An assessment of Antarctic Circumpolar Current and Southern Ocean meridional overturning circulation during 1958–2007 in a suite of interannual CORE-II simulations. *Ocean Modelling*, 94, 84–120. <https://doi.org/10.1016/j.ocemod.2015.07.009>
- Ferrari, R., Jansen, M. F., Adkins, J. F., Burke, A., Stewart, A. L., & Thompson, A. F. (2014). Antarctic sea ice control on ocean circulation in present and glacial climates. *Proceedings of the National Academy of Sciences of the United States of America*, 111(24), 8753–8758. <https://doi.org/10.1073/pnas.1323922111>
- Fox-Kemper, B., Adcroft, A. J., Böning, C. W., Chassignet, E. P., Curchitser, E. N., Danabasoglu, G., et al. (2019). Challenges and prospects in ocean circulation models. *Frontiers in Marine Science*, 6, 65. <https://doi.org/10.3389/fmars.2019.00065>
- Galbraith, E., & de Lavergne, C. (2019). Response of a comprehensive climate model to a broad range of external forcings: Relevant for deep ocean ventilation and the development of late cenozoic ice ages. *Climate Dynamics*, 52, 623–679. <https://doi.org/10.1007/s00382-018-4157-8>
- Gent, P. R., & Danabasoglu, G. (2011). Response to increasing southern hemisphere winds in CCSM4. *Journal of Climate*, 24, 4992–4998. <https://doi.org/10.1175/JCLI-D-10-05011.1>
- Gent, P. R., & McWilliams, J. C. (1990). Isopycnal mixing in ocean circulation models. *Journal of Physical Oceanography*, 20, 150–155. [https://doi.org/10.1175/1520-0485\(1990\)020<0150:imiocm>2.0.co;2](https://doi.org/10.1175/1520-0485(1990)020<0150:imiocm>2.0.co;2)
- Gent, P. R., Willebrand, J., McDougall, T. J., & McWilliams, J. C. (1995). Parameterizing eddy-induced tracer transports in ocean circulation models. *Journal of Physical Oceanography*, 25, 463–474. [https://doi.org/10.1175/1520-0485\(1995\)025<0463:peitti>2.0.co;2](https://doi.org/10.1175/1520-0485(1995)025<0463:peitti>2.0.co;2)
- Gill, A. E. (1982). *Atmospheric-Ocean dynamics*. Academic Press.
- Griffies, S. M. (1998). The Gent–McWilliams skew flux. *Journal of Physical Oceanography*, 28, 831–841. [https://doi.org/10.1175/1520-0485\(1998\)028<0831:tgmsf>2.0.co;2](https://doi.org/10.1175/1520-0485(1998)028<0831:tgmsf>2.0.co;2)
- Grooms, I. (2015). A computational study of turbulent kinetic energy transport in barotropic turbulence on the f -plane. *Physics of Fluids*, 27, 101701. <https://doi.org/10.1063/1.4934623>
- Hallberg, R., & Gnanadesikan, A. (2006). The role of eddies in determining the structure and response of the wind-driven Southern Hemisphere overturning: Results from the Modeling Eddies in the Southern Ocean (MESO) projects. *Journal of Physical Oceanography*, 36, 2232–2252. <https://doi.org/10.1175/JPO2980.1>
- Hofman, M., & Morales Maqueda, M. A. (2011). The response of Southern Ocean eddies to increased midlatitude westerlies: A non-eddy resolving model study. *Geophysical Research Letters*, 38, L03605. <https://doi.org/10.1029/2010GL045972>
- Hogg, A. M. (2010). An Antarctic Circumpolar Current driven by surface buoyancy forcing. *Geophysical Research Letters*, 37, L23601. <https://doi.org/10.1029/2010GL044777>
- Jansen, M. F. (2017). Glacial ocean circulation and stratification explained by reduced atmospheric temperature. *Proceedings of the National Academy of Sciences of the United States of America*, 114(1), 45–50. <https://doi.org/10.1073/pnas.1610438113>
- Jansen, M. F., Adcroft, A., Khani, S., & Kong, H. (2019). Toward an energetically consistent, resolution aware parameterization of ocean mesoscale eddies. *Journal of Advances in Modeling Earth Systems*, 1, 1–17. <https://doi.org/10.1029/2019MS001750>
- Jansen, M. F., Adcroft, A. J., Hallberg, R., & Held, I. M. (2015). Parameterization of eddy fluxes based on a mesoscale energy budget. *Ocean Modelling*, 92, 28–41. <https://doi.org/10.1016/j.ocemod.2015.05.007>
- Jansen, M. F., & Held, I. M. (2014). Parameterizing subgrid-scale eddy effects using energetically consistent backscatter. *Ocean Modelling*, 80, 36–48. <https://doi.org/10.1016/j.ocemod.2014.06.002>
- Jansen, M. F., Held, I. M., Adcroft, A. J., & Hallberg, R. (2015). Energy budget-based backscatter in an eddy permitting primitive equation model. *Ocean Modelling*, 92, 15–26. <https://doi.org/10.1016/j.ocemod.2015.07.015>
- Jones, C. S., & Abernathy, R. P. (2019). Isopycnal mixing controls deep ocean ventilation. *Geophysical Research Letters*, 46, 13144–13151. <https://doi.org/10.1029/2019GL085208>
- Kageyama, M., Braconnot, P., Harrison, S. P., Haywood, A. M., Jungclaus, J. H., Otto-Bliesner, B. L., et al. (2018). The PMIP4 contribution to CMIP6—Part 1: Overview and over-arching analysis plan. *Geoscientific Model Development*, 11(3), 1033–1057. <https://doi.org/10.5194/gmd-11-1033-2018>
- Klocker, A., & Marshall, D. P. (2014). Advection of baroclinic eddies by depth mean flow. *Geophysical Research Letters*, 41, L060001. <https://doi.org/10.1002/2014GL060001>
- Klöwer, M., Jansen, M. F., Claus, M., Greatbatch, R. J., & Thomsen, S. (2018). Energy budget-based backscatter in a shallow water model of a double gyre basin. *Ocean Modelling*, 132, 1–11. <https://doi.org/10.1016/j.ocemod.2018.09.006>
- Klymak, J. (2018). Non-propagating form drag and turbulence due to stratified flow over large-scale abyssal hill topography. *Journal of Physical Oceanography*, 48, 2383–2395. <https://doi.org/10.1175/JPO-D-17-0225.1>

- Klymak, J., Balwada, D., Naveira Garabato, A. C., & Abernathy, R. (2021). Parameterizing nonpropagating form drag over rough bathymetry. *Journal of Physical Oceanography*, 51, 1489–1501. <https://doi.org/10.1175/JPO-D-20-0112.1>
- Large, W. G., & Yeager, S. (2009). The global climatology of an interannually varying air-sea flux data set. *Climate Dynamics*, 33, 341–364. <https://doi.org/10.1007/s00382-008-0441-3>
- Levitus, S., Antonov, J. I., Boyer, T. P., Baranova, O. K., Garcia, H. E., Locarnini, R. A., et al. (2012). Work ocean hat content and thermosteric sea level change (0–2000 m), 1955–2010. *Geophysical Research Letters*, 39, L10603. <https://doi.org/10.1029/2012GL051106>
- Lin, X., Zhai, X., Wang, Z., & Munday, D. R. (2018). Mean, variability, and trend of Southern Ocean wind stress: Role of wind fluctuations. *Journal of Climate*, 31, 3557–3573. <https://doi.org/10.1175/JCLI-D-17-0481.1>
- Locarnini, R. A., Mishonov, A. V., Antonov, J. I., Boyer, T. P., Garcia, H. E., Baranova, O. K., et al. (2013). World ocean atlas 2013, volume 1: Temperature. In S. Levitus (Ed.), *Noaa atlas nesdis* (Vol. 73, pp. 1–40).
- MacKinnon, J. A., Alford, M. H., Ansong, J. K., Arbic, B. K., Barna, A., Briegleb, B. P., et al. (2017). Climate process team on internal-wave driven ocean mixing. *Journal of Fluid Mechanics*, 98, 2429–2454. <https://doi.org/10.1175/BAMS-D-16-0030.1>
- Maddison, J. R., & Marshall, D. P. (2013). The Eliassen–Palm flux tensor. *Journal of Fluid Mechanics*, 729, 69–102. <https://doi.org/10.1017/jfm.2013.259>
- Madec, G. (2008). *NEMO ocean engine*. Note du Pôle de modélisation, Institut Pierre-Simon Laplace (IPSL). No. 27.
- Madec, G., & Imbard, M. (1996). A global ocean mesh to overcome the North Pole singularity. *Climate Dynamics*, 12, 381–388. <https://doi.org/10.1007/BF00211684>
- Mak, J., Maddison, J. R., Marshall, D. P., & Munday, D. R. (2018). Implementation of a geometrically informed and energetically constrained mesoscale eddy parameterization in an ocean circulation model. *Journal of Physical Oceanography*, 48, 2363–2382. <https://doi.org/10.1175/JPO-D-18-0017.1>
- Mak, J., Marshall, D. P., Maddison, J. R., & Bachman, S. D. (2017). Emergent eddy saturation from an energy constrained parameterisation. *Ocean Modelling*, 112, 125–138. <https://doi.org/10.1016/j.ocemod.2017.02.007>
- Marshall, D. P., & Adcroft, A. J. (2010). Parameterization of ocean eddies: Potential vorticity mixing, energetics and Arnold's first stability theorem. *Ocean Modelling*, 32, 1571–1578. <https://doi.org/10.1016/j.ocemod.2010.02.001>
- Marshall, D. P., Ambaum, M. H. P., Maddison, J. R., Munday, D. R., & Novak, L. (2017). Eddy saturation and frictional control of the Antarctic circumpolar current. *Geophysical Research Letters*, 44, 286–292. <https://doi.org/10.1002/2016GL071702>
- Marshall, D. P., & Johnson, H. L. (2017). Relative strength of the Antarctic circumpolar current and Atlantic meridional overturning circulation. *Tellus*, 69, 1338884. <https://doi.org/10.1080/16000870.2017.1338884>
- Marshall, D. P., Maddison, J. R., & Berloff, P. S. (2012). A framework for parameterizing eddy potential vorticity fluxes. *Journal of Physical Oceanography*, 42, 539–557. <https://doi.org/10.1175/JPO-D-11-048.1>
- Melet, A., Hallberg, R., Adcroft, A., Nikurashin, M., & Legg, S. (2015). Energy flux into internal lee waves: Sensitivity to future climate changes using linear theory and a climate model. *Journal of Climate*, 28, 2365–2384. <https://doi.org/10.1175/JCLI-D-14-00432.1>
- Meredith, M. P., Garabato, A. C. N., Hogg, A. M., & Farneti, R. (2012). Sensitivity of the overturning circulation in the Southern Ocean to decadal changes in wind forcing. *Journal of Climate*, 25, 99–110. <https://doi.org/10.1175/2011JCLI4204.1>
- Meredith, M. P., & Hogg, A. M. (2006). Circumpolar response of Southern Ocean eddy activity to a change in the southern annular mode. *Geophysical Research Letters*, 33, L16608. <https://doi.org/10.1029/2006gl026499>
- Molemaker, M. J., McWilliams, J. C., & Yavneh, I. (2005). Baroclinic instability and loss of balance. *Journal of Physical Oceanography*, 35, 1505–1517. <https://doi.org/10.1175/JPO2770.1>
- Morrison, A. K., Hogg, A. M., & Ward, M. L. (2011). Sensitivity of the Southern Ocean overturning circulation to surface buoyancy forcing. *Geophysical Research Letters*, 38, L14602. <https://doi.org/10.1029/2011GL048031>
- Munday, D. R., Johnson, H. L., & Marshall, D. P. (2013). Eddy saturation of equilibrated circumpolar currents. *Journal of Physical Oceanography*, 43, 507–532. <https://doi.org/10.1175/JPO-D-12-095.1>
- Newman, L., Heil, P., Trebilco, R., Katsumata, K., Constable, A., van Wijk, E., et al. (2019). Delivering sustained, coordinated, and integrated observations of the Southern Ocean for global impact. *Frontiers in Marine Science*, 6, 433. <https://doi.org/10.3389/fmars.2019.00433>
- Ni, Q., Zhai, X., Wang, G., & Hughes, C. W. (2020). Widespread mesoscale dipoles in the global ocean. *Journal of Geophysical Research: Oceans*, 125, e2020JC016479. <https://doi.org/10.1029/2020JC016479>
- Ni, Q., Zhai, X., Wang, G., & Marshall, D. P. (2020). Random movement of mesoscale eddies in the global ocean. *Journal of Physical Oceanography*, 50, 2341–2357. <https://doi.org/10.1175/JPO-D-19-0192.1>
- Nikurashin, M., Vallis, G. K., & Adcroft, A. (2013). Routes to energy dissipation for geostrophic flows in the Southern Ocean. *Nature Geoscience*, 6, L08610. <https://doi.org/10.1038/NGEO1657>
- Perason, B., & Fox-Kemper, B. (2018). Log-normal turbulence dissipation in global ocean models. *Physical Review Letters*, 120, 094501. <https://doi.org/10.1103/PhysRevLett.120.094501>
- Poulsen, M. B., Jochum, M., Maddison, J. R., Marshall, D. P., & Nuterman, R. (2019). A geometric interpretation of Southern Ocean eddy form stress. *Journal of Physical Oceanography*, 49, 2553–2570. <https://doi.org/10.1175/JPO-D-18-0220.1>
- Pradal, M., & Gnanadesikan, A. (2014). How does the Redi parameter for mesoscale mixing impact global climate in an Earth system model? *Journal of Advances in Modeling Earth Systems*, 6, 586–601. <https://doi.org/10.1002/2013MS000273>
- Rai, S., Hecht, M., Maltrud, M. E., & Aluie, H. (2021). Scale of oceanic eddy killing by wind from global satellite observations. *Science Advances*, 7, eabf4920. <https://doi.org/10.1126/sciadv.abf4920>
- Rocha, C. B., Wagner, G. L., & Young, W. R. (2018). Stimulated generation: Extraction of energy from balanced flow by near-inertial waves. *Journal of Fluid Mechanics*, 847, 417–451. <https://doi.org/10.1017/jfm.2018.308>
- Roquet, F., Madec, G., McDougall, T. J., & Barker, P. M. (2015). Accurate polynomial expressions for the density and specific volume of seawater using the TEOS-10 standard. *Ocean Modelling*, 90, 29–43. <https://doi.org/10.1016/j.ocemod.2015.04.002>
- Rousset, C., Vancoppenolle, M., Madec, G., Fichefet, T., Flavoni, S., Barthélemy, A., et al. (2015). The Louvain-La-Neuve sea ice model LIM3.6: Global and regional capabilities. *Geoscientific Model Development*, 8, 2991–3005. <https://doi.org/10.5194/gmd-8-2991-2015>
- Ruan, X., Wenegrat, J. O., & Gula, J. (2021). Slippery bottom boundary layers: The loss of energy from the general circulation by bottom drag. *Geophysical Research Letters*, 48, e2021GL094434. <https://doi.org/10.1029/2021GL094434>
- Sen, A., Scott, R. B., & Arbic, B. K. (2008). Global energy dissipation rate of deep-ocean low-frequency flows by quadratic bottom boundary layer drag: Computations from current-meter data. *Geophysical Research Letters*, 35, L09606. <https://doi.org/10.1029/2008GL033407>
- Smith, K. S., & Marshall, J. (2009). Evidence for enhanced eddy mixing at middepth in the Southern Ocean. *Journal of Physical Oceanography*, 39, 50–69. <https://doi.org/10.1175/2008JPO3880.1>
- Sutherland, B. R., Achatz, U., Caulfield, C. P., & Klymak, J. M. (2019). Recent progress in modeling imbalance in the atmosphere and ocean. *Physical Review Fluids*, 4, 010501. <https://doi.org/10.1103/physrevfluids.4.010501>

- Takano, Y., Ito, T., & Deutsch, C. (2018). Projected centennial oxygen trends and their attribution to distinct ocean climate forcings. *Global Biogeochemical Cycles*, 32, 1329–1349. <https://doi.org/10.1029/2018GB005939>
- Toggweiler, J. R., Russel, J. L., & Carson, S. R. (2006). Midlatitude westerlies, atmospheric CO₂, and climate change during the ice ages. *Paleo-oceanography*, 21, PA2005. <https://doi.org/10.1029/2005PA001154>
- Toggweiler, J. R., & Samuels, B. (1995). Effect of Drake passage on the global thermohaline circulation. *Deep Sea Research Part 1: Oceanographic Research Papers*, 42(4), 477–500. [https://doi.org/10.1016/0967-0637\(95\)00012-U](https://doi.org/10.1016/0967-0637(95)00012-U)
- Viebahn, J., & Eden, C. (2012). Standing eddies in the meridional overturning circulation. *Journal of Physical Oceanography*, 42, 1496–1508. <https://doi.org/10.1175/JPO-D-11-087.1>
- Xu, C., Zhai, X., & Shang, X.-D. (2016). Work done by atmospheric winds on mesoscale ocean eddies. *Geophysical Research Letters*, 43, 12174–12180. <https://doi.org/10.1002/2016GL071275>
- Yang, L., Nikurashin, M., Hogg, A. M., & Sloyan, B. M. (2018). Energy loss from transient eddies due to lee wave generation in the Southern Ocean. *Journal of Physical Oceanography*, 48, 2867–2885. <https://doi.org/10.1175/JPO-D-18-0077.1>
- Zanna, L., Khatiwala, S., Gregory, J. M., Ison, J., & Heimbach, P. (2019). Global reconstruction of historical ocean heat storage and transport. *Proceedings of the National Academy of Sciences of the United States of America*, 116, 1126–1131. <https://doi.org/10.1073/pnas.1808838115>
- Zhang, Y., & Vallis, G. K. (2013). Ocean heat uptake in eddying and non-eddying ocean circulation models in a warming climate. *Journal of Physical Oceanography*, 43, 2211–2229. <https://doi.org/10.1175/JPO-D-12-078.1>
- Zweng, M. M., Reagan, J. R., Antonov, J. I., Locarnini, R. A., Mishonov, A. V., Boyer, T., et al. (2013). World ocean atlas 2013, volume 2: Salinity. In S. Levitus (Ed.). *Noaa atlas nesdis*, (Vol. 74, pp. 1–39).